Turkish J. Eng. Env. Sci.
26 (2002) , 293 – 300.

Experimental Analysis of Buried High Density Polyethylene Pipes

D. V. REDDY
Center for Marine Structures and Geotechnique, Department of Ocean Engineering, Florida Atlantic University, Boca Raton, 33431 FL, USA
Şenol ATAOĞLU
Faculty of Civil Engineering, Technical University of İstanbul, Maslak, 80626 İstanbul-TURKEY

Received 05.09.2000

Abstract

The primary goal of this study was to evaluate the deflections and bending moments of buried High density polyethylene (HDPE) pipes. The performance of buried HDPE pipes subjected to live loading was studied in soil chambers for three levels of service loading. Strains and diametral changes were measured for 10,000 hours. The discussion of the experimental findings is focused on certain recent concerns, associated with the HDPE piping related to deflection, longitudinal, and transverse stresses and bending moments. A 7.5% vertical change of diameter, which is the failure criterion, was observed at approximately 3,200 hours for the specimens heated at 50°C, and subjected to maximum service loading.

Key words: Infrastructure, Pipeline, Pipe-soil interaction, Viscoelasticity, HDPE

Introduction

The high-density polyethylene pipe has good potential for economic use for marine oil and gas pipelines, underdrains, storm sewers, culverts, and other subsurface drainage structures. In view of its inherent chemical and corrosion resistance, light weight, toughness, flexibility, easy splicing, and consequent easy handling and installation, HDPE piping is used extensively for gas pipelines. In the transportation industry, over forty states in the US use HDPE pipes as part of a 40% annual growth in the use of thermoplastic, HDPE and polyvinyl chloride (PVC) pipes in transportation construction projects (Goddard, 1995).

Experiments

Two types of corrugated HDPE pipe specimens of nominal inside diameters 305 mm were considered. Although there were small geometrical property differences between the two pipes, both have the same cell classification. Specifications of the materials are as follows:

Melt index: 0.4-0.15
Section area: 4.78-mm^2/mm
Cell classification: 335420C
Inside diameter: 305 mm (12 in.)
Outside diameter: 360.68 mm (14.2 in.)
Modulus of the pipe: 758 MPa (110 ksi)
Thickness (single wall): 3.2 mm (0.129 in.)
Weight [kg/6m(lb/20ft)]: 28.96 kg (63.8 lb)
Type of soil: ASTM D2321 Class II, SW/SP
Color and UV stabilizer: Black, 2% min. carbon
Density: 0.941, 0.955 g/cm^3(0.03397, 0.03448 lb/in^3)
Length of the pipe: 1981.2 mm (6′6”) corrugated (annular)
Tensile strength: 552-758 MPa (80000-110000psi) at yield
Moment of inertia: 0.574-0.522 cm^4/cm (0.035-0.0319 in.^{4}/in.) Type I-II
Load levels: M (maximum service load)=5600 lb, 3700 lb (2/3 M) and 1900 lb(1/3 M)

The experimental investigation addressed the changes in diameter and the strains of Type I and II buried pipes subjected to AASHTO loading. The long-term behavior was accelerated with super-ambient temperatures of 40 and 50°C to provide the data for life prediction at the ambient temperature of 20°C based on 7.5% vertical deflection as the failure criterion. Hence, readings were taken up to failure or 10,000 hours. The supports at the end of the pipe were located so that the bending effects could be eliminated.

Soil Chambers and Installation of the Measuring Devices

Each of the seven soil chambers was of 914.4 mm depth, 1980 mm length, and 3660 mm width. Every chamber was divided into four parts to accommodate four pipe specimens as shown in Figures 1 and 2. Pairs of specimens, notched (N) [Notch depth and length: 0.635 mm (0.025in.) and 7.94 mm (5/16 in.), ASTM 1474] and un-notched (U), were loaded simultaneously by using 2 channels 610 mm x 250 mm x 50 mm, to simulate a typical tire footprint, and a steel plate to distribute the load evenly, as shown in Figure 3. Four dial gages were mounted on the guide tubes of all specimens to measure the vertical and horizontal changes in the inside diameter at the mid-section, as shown in Figure 4. Only a few specimens were mounted with two strain gages, as shown in Figure 5, at the shoulders, located at 45° and 135° circumferentially and longitudinally, respectively. These locations correspond to the maximum stress locations (Ataoglu and Reddy, 2001, a-b). A third gage to measure longitudinal strain was located at the bottom.

Results of the Experimental Investigation

The experimental deflection data are presented for the pipes under different loadings and temperatures in Figures 6 to 19.

The experimental strain data and stresses are presented for Type I/II un-notched pipes under different loadings and temperatures in Reddy *et al.* (2001). Bending moments (M_0, lb in.) values are presented in Tables 1 to 7.

Figure 1. End view of the test set-up

Figure 2. Soil chambers (half full) after compaction

Figure 3. Set-up of structural sections for footprint loading

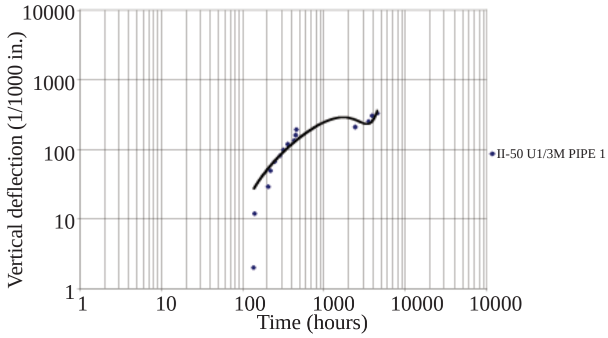

Figure 6. Change in diameter of Pipe 1

Figure 4. Set-up of dial gages

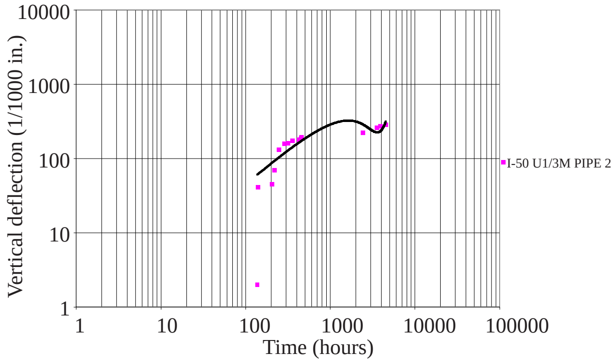

Figure 7. Change in diameter of Pipe 2

Figure 5. Reading of strain gages

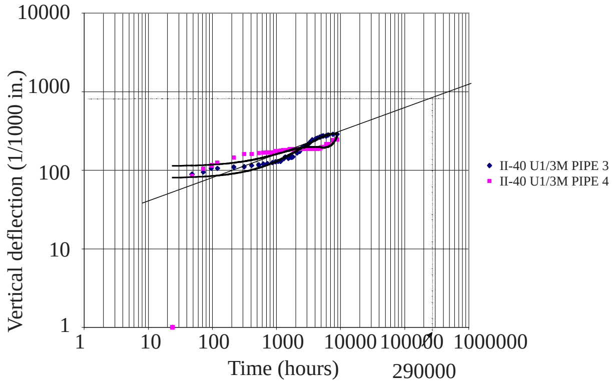

Figure 8. Change in diameter of Pipes 3 and 4

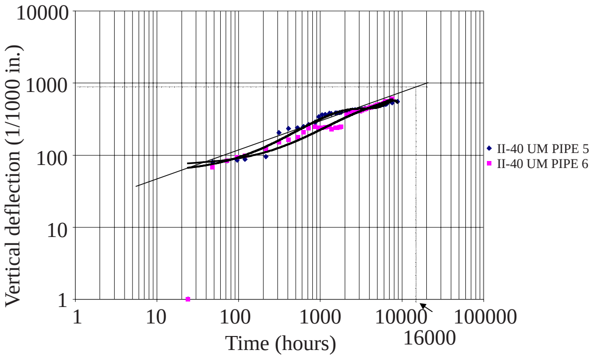

Figure 9. Change in diameter of Pipes 5 and 6

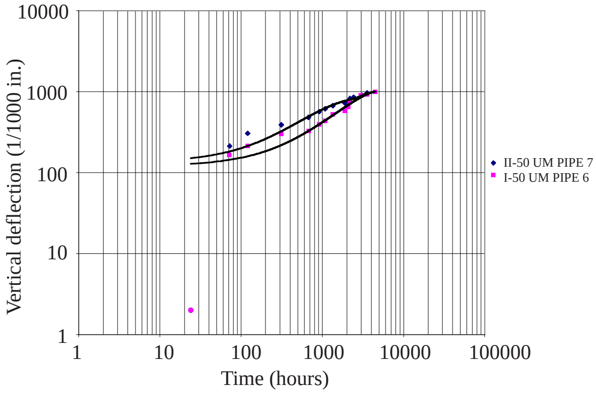

Figure 10. Change in diameter of Pipes 7 and 8

Table 1. Moments for Pipes 23, Load Applied (M), 40°C, I,U

Days	M_0 (45°)	M_0 (135°)	M_0 (270°)
1	0	0	0
6	0.292	228.44	131.7
9	1.843	321.58	138
16	3.011	419.15	141.1
19	4.48	530.61	151.3
24	5.71	654.59	159.7
27	6.151	713.21	193.4
39	7.14	906.01	234
41	7.758	1028.8	273.8
48	8.499	1080.6	324.5
56	9.207	1225	357.7
63	10.06	1279.5	436.2
72	10.91	1292.6	511.3
80	16.19	1335.2	556.8
88	18.84	1357.2	592.8
97	22.71	1473.7	623.8
103	24.68	1512.7	664.7
119	26.58	1565	735.3
126	28.74	1581.3	778.2
134	30.79	1655.1	833.4
149	31.72	1742.5	896.7
159	33.69	1828.5	946.8
185	35.18	1879.4	973.5
214	35.23	1818.3	1048
225	35.37	1906.2	1099
248	34.64	1876.4	1146
260	34.46	1924.7	1185
270	34.9	1956.9	1276
317	32.93	1864.9	1224
368	30.91	1756.8	1012

Table 2. Moments for Pipes 24, Load Applied (M), 40°C, I,U

Days	M_0 (45°)	M_0 (135°)	M_0 (270°)
1	0	0	0
6	7.03	196.24	122.3
9	8.561	289.39	226.5
16	9.683	387.2	177
19	11.13	498.78	208.3
24	12.33	623.01	261.4
27	12.75	681.63	294.8
39	13.66	874.92	334.1
41	14.26	997.56	373.6
48	14.96	1049.8	423.7
56	15.61	1194.4	456
63	16.41	1249.1	533.9
72	17.21	1262.5	608
80	22.43	1305.4	652.6
88	25.04	1327.5	687.9
97	28.84	1444.4	717.9
103	30.77	1483.6	758.2
119	32.57	1536.4	827.2
126	34.68	1552.9	869.4
134	36.67	1627	923.8
149	37.51	1714.8	985.5
159	39.41	1801.2	1035
185	40.72	1852.8	1059
214	40.59	1792.6	1131
225	40.65	1880.8	1181
248	39.76	1851.8	1225
260	39.51	1900.5	1262
270	39.88	1933.1	1352
317	37.6	1842.5	1295
368	35.24	1736.1	1078

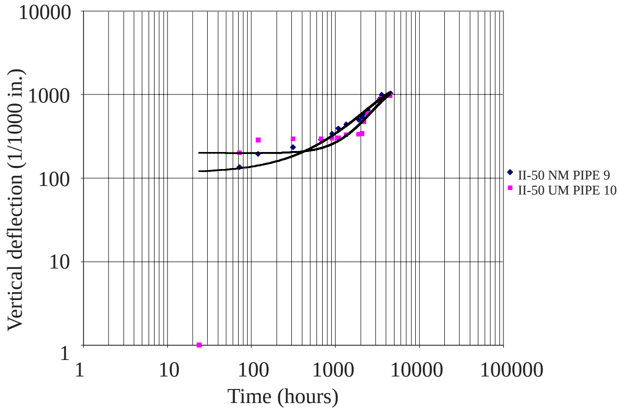

Figure 11. Change in diameter of Pipes 9 and 10

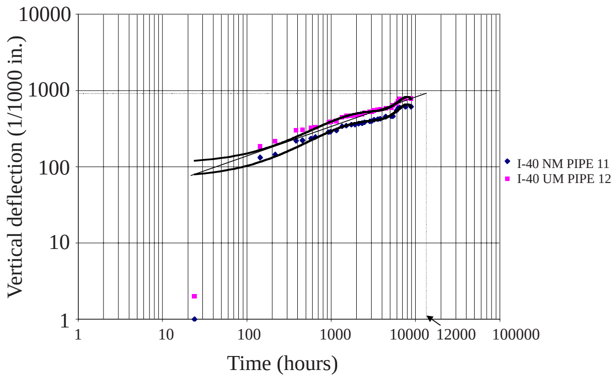

Figure 12. Change in diameter of Pipes 11 and 12

Table 3. Moments for Pipe 8, Load Applied (M) , 50°C, I,U

Days	M_0 (45°)	M_0 (135°)	M_0 (270°)
1	0.00	0	0
3	0.56	242.59	56.604
5	1.41	457.32	107.61
13	1.79	629.86	186.82
28	6.75	880.74	315.49
38	9.74	1014.9	442.43
45	11.53	1188.6	620.15
56	18.68	1354.0	651.47
79	26.59	1683.2	649.62
87	33.58	1922.3	729.39
91	38.03	2197.2	824.73
101	41.13	2246.5	840.19
124	42.65	2343.3	874.76
148	43.95	2368.3	1016.7
188	46.73	2347.7	1058.1

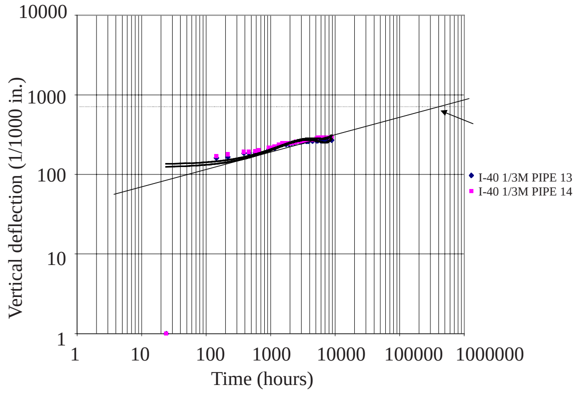

Figure 13. Change in diameter of Pipes 13 and 14

Table 4. Moments for Pipe 17, Load Applied (M), 20°C, II,U

Days	M_0 (45°)	M_0 (135°)	M_0 (270°)
1	0.00	0.00	0.00
6	1.26	226.51	54.68
9	2.75	334.87	176.00
16	3.87	448.56	119.10
19	5.28	578.29	155.75
24	6.45	722.70	217.88
27	6.88	790.89	257.00
39	7.82	1015.56	303.76
41	8.41	1158.28	349.90
48	9.11	1218.86	408.78
56	9.79	1387.02	446.99
63	10.60	1450.64	538.09
72	11.41	1466.18	625.03
80	16.48	1516.06	677.66
88	19.03	1541.90	719.26
97	22.73	1677.69	754.96
103	24.62	1723.27	802.31
119	26.44	1784.75	884.05
126	28.50	1803.91	933.63
134	30.47	1890.09	997.59
149	31.36	1992.19	1070.55
159	33.24	2092.61	1128.52
185	34.64	2152.76	1158.69
214	34.67	2082.83	1244.98
225	34.79	2185.35	1303.86
248	34.06	2151.73	1357.61
260	33.88	2208.33	1402.00
270	34.29	2246.20	1507.09
317	32.35	2140.87	1446.01
368	30.36	2017.35	1197.36

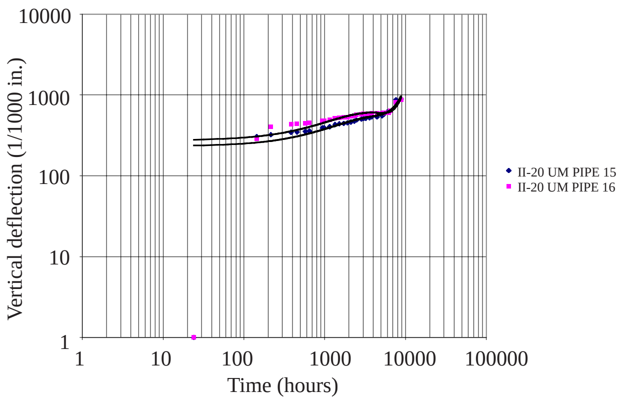

Figure 14. Change in diameter of Pipes 15 and 16

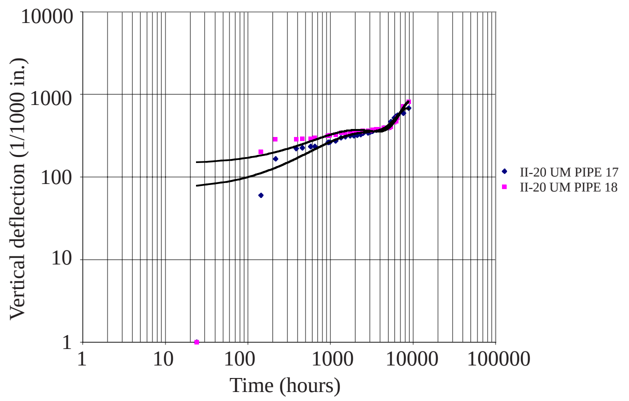

Figure 15. Change in diameter of Pipes 17 and 18

Table 5. Moments for Pipe 18, Load Applied (M), 20°C, II,U

Days	M_0 (45°)	M_0 (135°)	M_0 (270°)
1	0	0	0
6	0.99	151.53	15.62
9	2.479	260.11	23.36
16	3.598	374.31	27.84
19	5.009	504.27	40.09
24	6.189	649.05	50.64
27	6.611	717.46	90.26
39	7.554	943.02	139
41	8.147	1085.9	185.5
48	8.854	1147	245.6
56	9.53	1315.7	285.1
63	10.34	1379.9	377.4
72	11.16	1396.1	465.8
80	16.23	1446.6	519.8
88	18.78	1473	562.8
97	22.49	1609.4	600
103	24.38	1655.5	648.3
119	26.2	1718.1	732.8
126	28.27	1737.8	783.5
134	30.23	1824.6	848.8
149	31.12	1927.8	924.3
159	33.01	2029	984
185	34.42	2091	1019
214	34.46	2023.2	1110
225	34.58	2126.6	1170
248	33.86	2094.7	1228
260	33.68	2152.2	1274
270	34.1	2190.8	1381
317	32.94	2088.9	1328
368	32.38	1969.2	1088

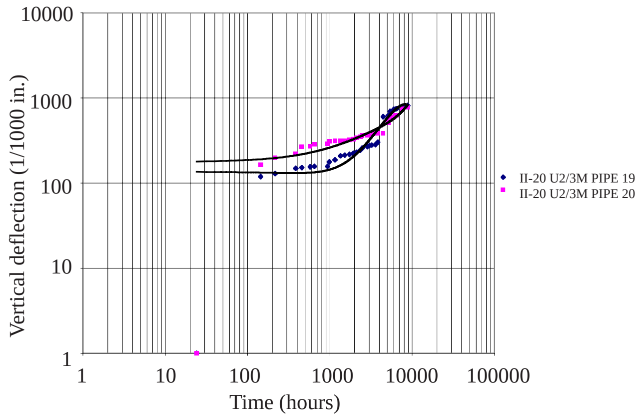

Figure 16. Change in diameter of Pipes 19 and 20

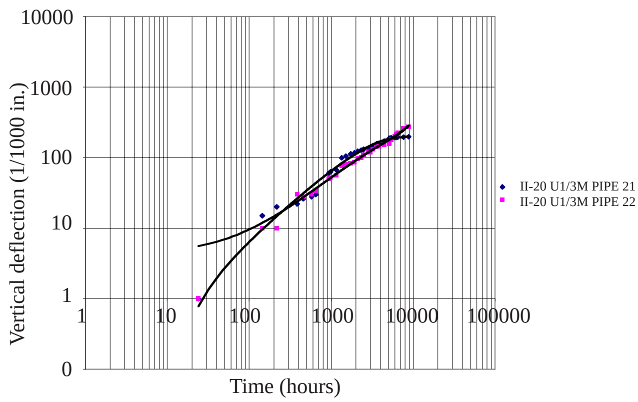

Figure 17. Change in diameter of Pipes 21 and 22

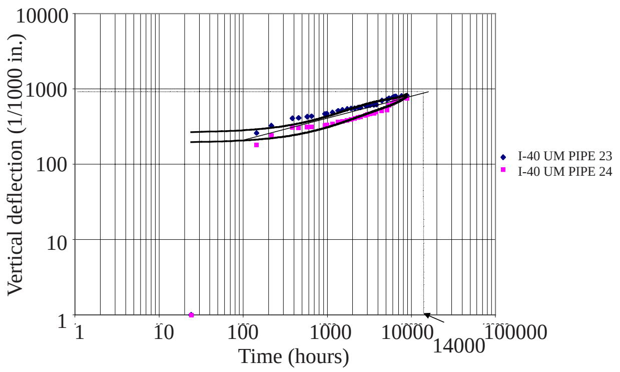

Figure 18. Change in diameter of Pipes 23 and 24

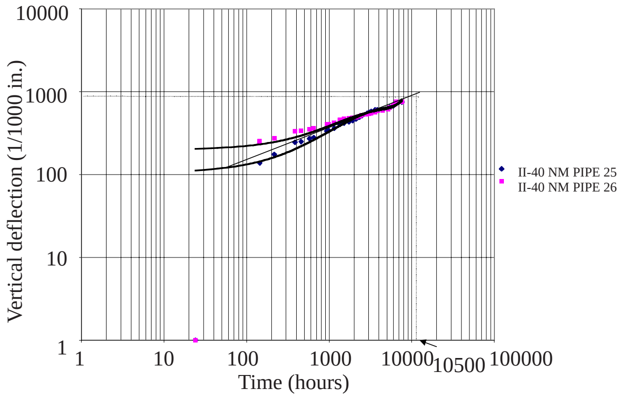

Figure 19. Change in diameter of Pipes 25 and 26

Table 6. Moments for Pipe 1, Load Applied (M/3), 50°C, II,U

Days	M_0 (45°)	M_0 (135°)	M_0 (270°)
1	0	0	0
3	0.15	21.93	114.37
5	0.48	131.35	187.64
13	3.08	394.04	201.67
28	4.21	449.29	209.36
38	5.63	780.60	211.79
45	6.49	590.28	310.91
56	8.02	613.31	326.70
79	8.52	660.99	358.03
87	9.52	685.54	416.78
91	10.23	734.11	453.63
101	11.62	772.91	509.61
148	12.12	813.90	573.49
162	12.62	876.14	594.66
188	12.36	922.58	586.86

The maximum effective stress was 2.614 MPa (379.17 psi), (i.e. 7.5% deflection of the diameter), which is much less than 20.68 MPa (3000 psi), which is the Corrugated Polyethylene Pipe Association (CPPA) yield stress (Reddy *et al.*, (2001). The change in diameter is the governing factor and the CPPA limit is not reasonable for the general failure criterion of the buried HDPE pipe subjected to live loading.

Conclusions

The discussion of the experimental findings is focused on the HDPE piping related to deflections, stresses, and bending moments. H-20 truck loading was used to determine the maximum allowable loading of the specimens. The actual loading of most of the vehicles is less severe than that for the H-20 truck specification. In view of the strong time and temperature dependence of polyethylene, exposure to super-ambient temperatures was used to accelerate the failure mechanisms for service life prediction of the viscoelastic HDPE pipe. A 7.5% vertical change in diameter (the failure criterion) and bending were observed. A 7.5% vertical change in diameter was observed for the specimens heated to 50°C, with the maximum loading. Life prediction was determined from the Arrhenius equation and the Bi-directional Shifting Function method (BSM). Both methods gave similar life predictions, as shown in Table 8, but the BSM was more conservative (Reddy *et al.*, 2001). A 7.5% vertical change in diameter, or more, was observed at approximately 3,200 hours for the specimens heated at 50°C, and subjected to maximum loading. A 6 to 7% vertical change of diameter was observed at 10,000 hours for the specimens heated at 40°C and subjected to maximum loading. Therefore, extrapolation had to be performed for this temperature environment to determine the corresponding time of failure (7.5% vertical change in diameter). From these values, life prediction at ambient temperatures (20°C), based on vertical changes of diameter, was performed. Notches accelerated the vertical changes in diameter, but no creep-rupture was observed within the time frame of 10,000 hours. The maximum service lives for specimens at ambient temperature and subjected to maximum loading were approximately 30 and 80 years for notched/unnotched specimens, respectively, assuming proper installation and 90% compaction.

Table 7. Moments for Pipe 7, Load Applied (M), 50°C, II,U

Days	M_0 (45°)	M_0 (135°)	M_0 (270°)
1	0.00	0.00	0.00
3	0.21	81.47	50.14
5	1.02	193.90	131.35
13	1.40	260.63	245.12
28	6.18	327.04	409.57
38	9.05	521.92	521.92
45	10.77	632.34	735.98
56	17.66	871.71	744.00
79	25.28	1098.75	755.21
87	32.00	1329.41	840.76
91	36.28	1438.18	944.48
101	39.26	1769.50	1111.25
148	40.74	1948.81	1193.99
162	41.99	2175.80	1316.22
188	44.68	2152.70	1307.00

For HDPE piping, the yield stress should not exceed 20.68 MPa (3000 psi). Test results indicated that the maximum stress is at the shoulder, and is much less than the CPPA limit (Reddy *et al.*, 2001).

The CPPA limit (3000 psi), which is based on yielding due to the bending, is not reasonable for the general failure criterion of the buried HDPE pipe subjected to live loading. The deflection threshold seems to be the governing failure criterion.

Table 8. Comparison of the Arrhenius and the Bi-directional Methods

Type	Arrhenius (years)	Bi-directional (years)
I-NM	32.6	31.9
I-UM	81.5	91.3
I-U1/3	1,141	1,712
II-NM	25.4	28.5
II-UM	76.1	78.7
II-U1/3	1,130	1,027.4

Acknowledgements

The authors would like to thank the Florida Department of Transportation (Contract Monitor: Mr. R. G. Powers, Material Division) for financial support. Thanks are also due to Dr. S.E. Dunn, Professor and former Chairman, Department of Ocean Engineering, and Dr. J.S. Jurewicz, Dean of Engineering, Florida Atlantic University, for their support and encouragement.

References

Ataoglu, S., and Reddy, D.V., "Boundary Element Analysis of Buried Pipe-Soil Interaction", Proceedings of the 14th International Conference on Boundary Element Technology, (eds. Kassab, A., & Brebbia, C. A.), Witpress, Orlando, FL, 195-205, 2001.

Ataoglu, S., and Reddy, D.V., "Boundary Element Analysis of Pipe-Soil Interaction", 18th Canadian Congress of Applied Mechanics, (eds. Swamidas, A., Haddara, M.R., and Seshadri, R.), MUN, St. John's, NF, 237-238, 2001.

Goddard, J.B., "Research Problem Statement for TRB Committee A2C06 on Culverts and Hydraulic Structures", 1995.

Reddy, D.V., Gazagnaire, C., Ataoglu, S., and Powers, R., "Analysis of HDPE Pipe-Compacted Soil Interaction", Proceedings of the 33rd International SAMPE Conference, Seattle, WA, 494-505, 2001.